Role of the N-Terminal Hydrophilic Domain of Acyl-Coenzyme A:Cholesterol Acyltransferase 1 on the Enzyme's Quaternary Structure and Catalytic Efficiency[†]

Chunjiang Yu, Yi Zhang, Xiaohui Lu, Jun Chen, Catherine C. Y. Chang, and Ta-Yuan Chang*

Biochemistry Department, Dartmouth Medical School, Hanover, New Hampshire 03755

Received November 2, 2001

ABSTRACT: Acyl-coenzyme A:cholesterol acyltransferase (ACAT) is an enzyme involved in cellular cholesterol homeostasis and atherosclerosis. ACAT1 is an allosteric enzyme responding to its substrate cholesterol in a sigmoidal manner. It is a homotetrameric protein that spans the membrane multiple times, with its N-terminal 131 hydrophilic amino acids residing at the cytoplasmic side of the endoplasmic reticulum. This region contains two closely linked putative α-helices. Our current studies show that this region contains a dimer-forming motif. Adding this motif to the bacterial glutathione *S*-transferase (GST) converted the homodimeric GST to a tetrameric fusion protein. Conversely, deleting this motif from the full-length ACAT1 converted the enzyme from a homotetramer to a homodimer. The dimeric ACAT1 remains enzymatically active. Its biochemical characteristics, including the sigmoidal response to cholesterol, the IC_{50} value toward a specific ACAT inhibitor, and sensitivity toward heat inactivation, are essentially unaltered. On the other hand, the dimeric ACAT1 exhibits a 5−10-fold increase in the V_{max} of the overall reaction and a 2.2-fold increase in the K_m for oleoyl-coenzyme. Thus, deleting the dimer-forming motif near the N-terminus changes ACAT1 from its tetrameric form to a dimeric form and increases its catalytic efficiency.

Acyl-coenzyme A:cholesterol acyltransferase[1] (ACAT) is an enzyme present ubiquitously in various eukaryotic cells. In mammalian cells, it utilizes fatty acyl-coenzyme A and cholesterol present in the endoplasmic reticulum (ER) as substrates to produce cholesteryl esters (reviewed in ref *1*). Within cells, cholesteryl esters exist mainly as cytoplasmic lipid storage droplets. In plasma lipoproteins (very low density lipoproteins and chylomicrons), cholesteryl esters constitute part of the core lipid. In addition, cholesteryl esters accumulate in cellular lesions within the aortic blood vessels during the early stages of the disease atherosclerosis. For these reasons, ACAT has been identified as a potential pharmaceutical target for therapeutic intervention of atherosclerosis (reviewed in ref *2*). In addition, a recent study demonstrates that inhibiting ACAT activity attenuates the production of β-amyloid peptide in various cell types, raising the possibility that ACAT inhibitors may serve as useful therapeutic agents for treating patients with Alzheimer's disease (*3*). The first ACAT gene (*ACAT1*) was identified in 1993 (*4*). More recently, a similar but different ACAT gene (*ACAT2*) has also been identified in various mammalian species (*5*−*7*). Extensive sequence homology exists between ACAT1 and ACAT2 near their C-termini but not near their N-termini. In adult humans, results suggest that ACAT1 is the major enzyme in a variety of tissues including liver, adrenal glands, kidney, and macrophages, while ACAT2 is the major enzyme in the villi of the small intestines (*8*−*10*; reviewed in ref *11*). In hepatocyte-like HepG2 cells, both ACAT1 and ACAT2 were present (*8*); free fatty acids added in the growth medium of HepG2 cells were shown to increase the mRNA levels of ACAT1 but not ACAT2 (*12*). At present, there is good evidence implicating the role of ACAT1 in macrophage foam cell formation and ACAT2 in intestinal cholesterol absorption. On the other hand, the roles of ACAT1 and ACAT2 in the lipoprotein assembly process are less clear (*11*, *13*). With regard to the ACAT active site, it has been proposed by various investigators that a conserved serine and a conserved histidine (S269 and H460 in human ACAT1) constitute part(s) of the ACAT active site (*13*−*16*). The functions of these residues are unknown at present. The His460 is within a long hydrophobic region that comprises more than 20 amino acids. It has been postulated that part of this hydrophobic peptide segment may reside within the lipid bilayer, allowing the enzyme to produce cholesteryl esters in situ (*17*). In addition, Guo and colleagues recently proposed that several residues may constitute part of the ACAT substrate binding site(s) (*18*).

We have previously shown that recombinant ACAT1 expressed in CHO cells or in insect H5 cells could be purified extensively to electrophoretic homogeneity with retention of catalytic function (*16*, *19*). Purified ACAT1 present in vesicles or in mixed micelles responds to cholesterol as its substrate in a sigmoidal manner, implying that ACAT1 is an allosteric enzyme regulated by its own substrate cholesterol (*19*). To our knowledge, this is the first report demonstrating an allosteric effect on a membrane-bound enzyme by its lipophilic substrate. The molecular basis that

[†] This work is supported by NIH Grant HL 60306 (to T.-Y.C.).

* Corresponding author. Fax: 603-650-1128. Tel: 603-650-1622. E-mail: Ta.Yuan.Chang@Dartmouth.Edu.

[1] Abbreviations: ACAT, acyl-coenzyme A:cholesterol acyltransferase; aa, amino acid; BMH, bis(maleimidohexane); BSA, bovine serum albumin; CHO, Chinese hamster ovary; DSS, disuccinimidyl suberate; ER, endoplasmic reticulum; GST, glutathione *S*-transferase; H5, High Five; PBS, phosphate-buffered saline; SDS−PAGE, sodium dodecyl sulfate−polyacrylamide gel electrophoresis.

10.1021/bi0120188 CCC: $22.00
Published on Web 02/22/2002

controls the ACAT1 allosterism, as well as the catalytic mechanism of the enzyme, is essentially unknown at present. Our current goal is to identify the structural motif(s) that govern(s) the oligomerization state of ACAT1 and to examine whether altering the oligomerization state of the enzyme may affect its allosteric property, as well as its catalytic function. Depending on the methods used, ACAT1 in transfectant cells was shown to span the ER membrane seven times (*20*) or five times (*21*), with the first 131 hydrophilic amino acids residing on the cytoplasmic side of the ER. On the basis of results from hydrodynamic analysis, chemical cross-linking studies, and immunoprecipitation studies, ACAT1 was shown to contain four identical subunits in vitro and in intact cells (*22*). The protein secondary structure prediction program (*23*, *24*) has revealed the potential existence, between amino acids 43−99 of human ACAT1, of two closely linked helices followed by a short, β-sheet structure. In this paper, we examined the possible importance of this region in contributing to the structural integrity and enzymatic function of ACAT1. We produced various bacterial glutathione *S*-transferase (GST)−ACAT1 N-terminal peptide fusion proteins and examined their sizes. The same strategy was employed by other investigators to demonstrate various functional domains within a given protein (*25*, *26*). We also performed site-specific mutagenesis experiments on the GST-ACAT1 N-terminal peptide fusion protein construct, and the full-length ACAT1 cDNA. The results indicate that the helix-rich region (aa 43−84) contains a dimer-forming motif. Disrupting this motif from the full-length ACAT1 converts the enzyme to a homodimer that is more catalytically active than the native homotetramer. On the other hand, the dimeric enzyme responds to cholesterol in essentially the same manner as the tetrameric enzyme. Therefore, the tetrameric form is not required for ACAT1 to behave as an allosteric enzyme.

EXPERIMENTAL PROCEDURES

Materials. Bacterial expression vectors pGEX3X and pGEX2T and glutathione−Sepharose beads for GST fusion protein purification were from Pharmacia, Inc. Cysteine-specific cross-linking reagent bis(maleimidohexane) (BMH) and disuccinimidyl suberate (DSS) were from Pierce. Other materials used have been described previously (*19*, *22*, *27*).

Methods. Standard recombinant DNA techniques used were as described (*28*).

GST-ACAT1 Peptide Fusion Proteins. Methods for producing various GST-ACAT1 peptide fusion proteins were described in the instruction manual from Pharmacia. The construct pGST3X-ACAT1$_{1-131}$ was described previously (*27*). To produce the constructs pGST3X-ACAT1$_{1-63}$ and pGST2T-ACAT1$_{1-101}$, DNA fragments corresponding to the appropriate ACAT1 peptide sequences were PCR amplified from the DNA template pGST3X-ACAT1$_{1-131}$ using a common forward primer 5′-d(GGGCTGGCAAGCCACGTTTG-GTG)-3′ with a *Bam*HI site at the 5′-end and various appropriate reverse primers with an *Eco*RI site at their 3′-ends. The PCR products were cleaved with *Bam*HI and *Eco*RI and ligated into vector pGST3X or vector pGST2T cleaved with *Bam*HI and *Eco*RI. To create pGST3X-ACAT1$_{1-54}$, ACAT1$_{1-54}$ DNA fragment was released from the construct pGST3X-ACAT1$_{1-131}$ with *Bam*HI and *Hin*cII and then ligated with the vector pGST3X digested with *Bam*HI and *Sma*I. To create pGST2T-ACAT1$_{55-131}$, ACAT1$_{55-131}$ DNA fragment was released from the construct pGST3X-ACAT1$_{1-131}$ with *Hin*cII and *Eco*RI and then ligated with the vector pGST2T digested with *Sma*I and *Eco*RI.

Double or Single Proline Mutants Derived from pGST-ACAT1$_{1-131}$. These mutants were created by site-directed mutagenesis using the QuikChange method (Stratagene). The following forward and reverse primer pairs were used: for the P28,29 mutant, 5′-(CAG-AGA-AAC-CCT-CCA-AAG-GAG-TCC)-3′ and 5′-(GGA-CTC-CTT-TGG-AGG-GTT-TCT-CTG)-3′; for the P47,48 mutant, 5′-(GAC-ATA-AAA-CAG-TTG-CCA-CCA-AAG-AAG-ATA-AAG)-3′ and 5′-(CTT-TAT-CTT-CTT-TGG-TGG-CAA-CTG-TTT-TAT-GTC)-3′; for the P64 mutant, 5′-(G-GAA-TTG-AAG-CCA-CCT-TTT-ATG-AAG-GAA-G)-3′ and 5′-(C-TTC-CTT-CAT-AAA-AGG-TGG-CTT-CAA-TTC-C)-3′; for the P95,96 mutant, 5′-(GGG-TGC-GCT-CTC-CCA-CCC-TTT-TCT-GTT-CTT-G)-3′ and 5′-(C-AAG-AAC-AGA-AAA-GGG-TGG-GAG-AGC-GCA-CCC)-3′.

Expression and Size Analyses of GST-ACAT1 Fusion Proteins. Expression of GST-ACAT1 peptide fusion proteins in *Escherichia coli* BL21 was described in the instruction manual from Pharmacia. To briefly describe the GST-ACAT1 peptide fusion protein purification procedure, the *E. coli* cell pellets were gently washed with ice-cold PBS and sonicated in the lysis buffer (5 μM leupeptin, 2 mM PMSF, 5 mM EDTA, 5 mM DTT, and 0.25% Sarkosyl, in cold PBS). The lysate was cleared by centrifugation at 10000 rpm for 10 min at 4 °C, filtered through a 0.8 μm filter, and then loaded onto a 1 × 3 cm glutathione−Sepharose 4B column at 4 °C. The flow-through was loaded once more. The column was washed with prelysis buffer, and the GST-ACAT1 peptide fusion protein was eluted with 20 mL of the elution buffer (50 mM Tris, 10 mM glutathione, 10 mM DTT, 5 mM EDTA, 0.1 M NaCl, pH 8.0). The molecular masses of GST-ACAT1 peptide fusion proteins were estimated by ultracentrifugation or by gel filtration chromatography using various protein standards as molecular mass markers, based on procedures described previously (*22*) with some modification. Briefly, a 3 mL 5−20% linear sucrose gradient was prepared in buffer A (50 mM Tris, pH 7.8, 5 mM EDTA) in an SW60 Ultra-Clear tube (Beckman no. 344062). Protein samples with 25 mM DTT in buffer A were cleared by centrifugation at 4 °C in a 50Ti rotor at 40000 rpm for 35 min. Then 200 μL of the cleared sample was loaded on top of each gradient. Centrifugation was at 340000*g* for 12 h at 4 °C in a Beckman SW60 rotor. Fractions were subjected to Western blot analysis with ACAT1-specific antibodies DM10. To perform gel filtration chromatography for GST-ACAT1 peptide fusion proteins, a 90 × 1.6 cm column was packed with Sephacryl S-200 in buffer A. Fractions were collected at 1.1 mL per fraction and subjected to Western blot analysis with the ACAT1 antibodies DM10.

Mutant Constructs Derived from pHisACAT1. The recombinant plasmid pHisACAT1 was described previously (*19*). It contains a six-histidine tag (that functions as a metal binding domain), a T7 antigenic tag, an enterokinase cleavage recognition site, and the coding sequence of human ACAT1 with the first methionine converted to leucine. This construct was used to generate the HisACAT1 virus using the

baculovirus-insect cell technology (Invitrogen) (*19*, *29*). To produce the construct HisACAT1/Δ1−65, the 66th aa of *ACAT1* cDNA in *Puc 19* was mutated from Met to Leu (ATG to CTT) by site-specific mutagenesis, introducing an *Afl*II site. The DNA fragment that encodes $ACAT1_{66-550}$ was released by *Afl*II and *Hin*dIII and then inserted into the pBlueBacHisC vector (Invitrogen). The resultant plasmid HisACAT1/Δ1−65 was used to generate the HisACAT1/Δ1−65 virus for insect High Five (H5) cell expression or was inserted into the expression vector in pcDNA3 (Invitrogen) for mammalian cell expression. To produce the construct HisACAT1/p64, site-specific mutagenesis was performed using the construct HisACAT1 in pcDNA3 (*19*), using the QuikChange method with the following pair of primers: forward primer *5′*-(G-GAA-TTG-AAG-CCA-CCT-TTT-ATG-AAG-GAA-G)-*3′* and reverse primer *5′*-(C-TTC-CTT-CAT-AAA-AGG-TGG-CTT-CAA-TTC-C)-*3′*. The resultant construct was used to generate the HisACAT1/p64 virus for insect cell expression. Coding sequences for all of the constructs described were verified by automated cycling sequencing.

Purification and Size Analyses of Various HisACAT1 Mutants. Various recombinant HisACAT1s expressed in infected H5 cells were partially purified using the Talon Superflow resin from Clontech. Briefly, 80−90% confluent insect H5 cells grown in ten 150 mm dishes were infected by the individual recombinant ACAT1 baculovirus for 48 h. The cells were gently rinsed with cold PBS twice and then harvested by the hypotonic shock-scraping method (*30*) in 0.5 mL/150 mm dish of 50 mM Tris, pH 7.8, with protease inhibitors (2 μg/mL aprotinin, 2 μg/mL antipain, 0.1 μg/mL chymostatin, and 0.5 μg/mL leupeptin). The cell extracts were solubilized with 2% CHAPS, 1 M KCl, and 50 mM Tris, pH 7.8 (*19*), and centrifuged at 100000*g* for 45 min. The solubilized enzyme was then transferred into a tube containing 5 mL of Talon beads preequilibrated with buffer (50 mM Tris, 1 M KCl, and 1% CHAPS, with protease inhibitors indicated above, pH 7.8). The mixture was gently mixed in the cold room for 20 min. The beads were pelleted by a 2 min spin in a microfuge and then washed three times with 10 mL/wash of wash buffer (20 mM imidazole, 50 mM Tris, 1 M KCl, 1% CHAPS, pH 7.8); each wash consisted of gentle mixing for 2 min at 4 °C. The beads were resuspended in 6 mL of the wash buffer and transferred to a clear 1.0 × 10 cm column. The packed column was eluted with 10 mL of wash buffer and then eluted with 7 mL of 500 mM imidazole, 50 mM Tris, 1 M KCl, and 0.5% CHAPS, pH 7.8. The eluents were collected at 1 mL/fraction in siliconized tubes and then stored at −80 °C. The ACAT activity usually emerged at fraction 3, and peaked at fraction 4 or 5. On average, this procedure gave a 20−30-fold purification in ACAT specific activity with 30−40% activity recovery. Only the fraction that contained the peak ACAT activity was employed for biochemical analysis. Ultracentrifugations and gel filtrations in detergents and methods for estimating protein molecular masses were according to procedures previously described (*22*).

Chemical Cross-Linking Experiments. The experiments were conducted according to procedures described previously (*16*, *22*) using intact H5 cells expressing high levels of HisACAT1, HisACAT1/P64, or HisACAT1/Δ1−65. The primary amine-specific cross-linker DSS was used.

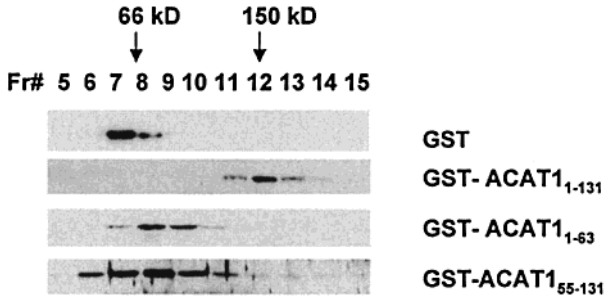

FIGURE 1: Sucrose density gradient velocity centrifugation analysis of affinity-purified GST and various GST-ACAT1 fusion proteins. GST or various GST-ACAT1 fusion proteins as indicated were purified with glutathione−Sepharose beads. Purified proteins at approximately 0.1−0.5 mg/mL were loaded atop a 5−20% linear sucrose gradient and centrifuged for 12 h at 50000 rpm at 4 °C in a Beckman SW60 rotor. For each sample, fifteen 200 μL fractions were collected from the top to the bottom. The fractions were subjected to 12.5% SDS−PAGE. Western blots were performed with ACAT-specific antibodies or with GST-specific antibodies. Arrows indicate the migration peaks of bovine serum albumin (66 kDa) and yeast alcohol dehydrogenase (150 kDa). Rows (from top to bottom): GST alone; GST-$ACAT1_{1-131}$; GST-$ACAT1_{1-63}$; GST-$ACAT1_{55-131}$. The results represent one of two independent experiments.

RESULTS

Size Analysis of Various GST-ACAT1 Peptide Fusion Proteins. ACAT1 is a homotetrameric protein. We reasoned that the helix-rich region near the N-terminus of ACAT1, between amino acids 43−99, may contain an oligomerization motif. To test this possibility, we constructed three fusion proteins by fusing each of the three overlapping ACAT1 peptides (aa 1−63, 1−131, and 55−131) to the bacterial glutathione *S*-transferase (GST). These GST fusion proteins were expressed at high levels in *E. coli*. The molecular masses of these fusion proteins were analyzed by sucrose density gradient velocity ultracentrifugation. The results show (Figure 1) that the GST exhibits a molecular mass of 55 kDa (first row). Since the monomer molecular mass of GST is 26 kDa (*31*), GST in solution is a dimer as expected. The GST-$ACAT1_{1-131}$, with an expected monomer molecular mass at 41 kDa, exhibits a molecular mass of about 160 kDa (second row); thus it is a tetramer.[2] Additional experiments show that the GST-$ACAT1_{1-101}$ fusion protein also behaves as a tetramer in solution (result not shown). Other results (Figure 1, third and fourth rows) show that both the GST-$ACAT1_{1-63}$, with its expected monomer molecular mass at 33 kDa, and the GST-$ACAT1_{55-131}$, with its expected monomer molecular mass at 35 kDa, exhibit a molecular mass of 70 kDa. Thus, both fusion proteins in solution behave as dimers. Overall, these results suggest that the peptide sequence in $ACAT1_{1-131}$ contains a dimer-forming domain; this motif is disrupted in $ACAT1_{1-63}$ or in $ACAT1_{55-131}$. According to the PhD protein secondary structure prediction program (*23*, *24*), the $ACAT1_{1-101}$ peptide may contain two closely linked α-helices within aa 43−84 (indicated with two closely linked double underlines in Figure 2A) and a β-sheet within aa 93−99 (indicated with a single underline in Figure

[2] In additional experiments, we performed gel filtration chromatography using Sephacryl S-200 and found that the molecular mass of GST in solution is 55 kDa and that the molecular mass of GST-$ACAT1_{1-131}$ in solution is 160 kDa (results not shown).

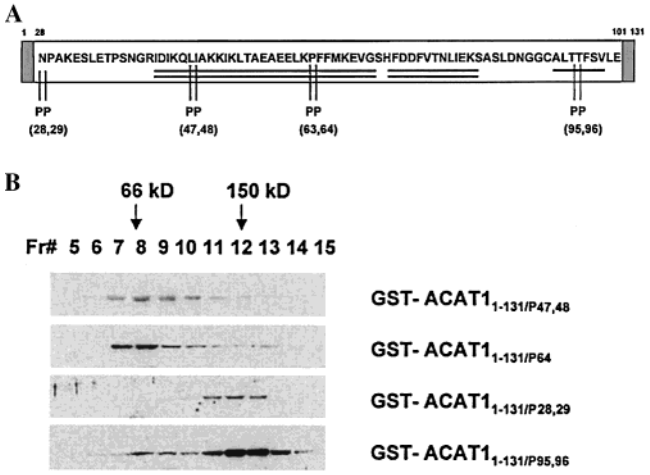

FIGURE 2: (A) The aa sequence of human ACAT1 from residues 28−101. The putative helix-rich region is indicated by two closely linked double underlines. The putative β-sheet region is indicated by a short single underline. The positions of the four individual double or single proline substitution mutations produced within GST-ACAT1$_{1-131}$ are also indicated. See text for details. (B) Sucrose density gradient velocity centrifugation analysis of various affinity-purified GST-ACAT1 fusion proteins. The experiments were performed in the same manner as described in Figure 1. Rows (from top to bottom): GST-ACAT1$_{1-131/P47,48}$; GST-ACAT1$_{1-131/P64}$; GST-ACAT1$_{1-131/P28,29;}$ GST-ACAT1$_{1-131/P95,96}$.

2A.). Prolines are known to be secondary structure breakers (*32*). Inserting a proline immediately before or within the coiled-coil domain may cause the coils to be out of phase with each other. Double proline mutations may be even more effective than single proline mutations. Proline(s) can also disrupt the β-sheet domain. To further analyze the putative dimer-forming domain within the ACAT1$_{1-131}$, we engineered four site-specific mutant GST-ACAT1$_{1-131}$ constructs, containing prolines at position 28, positions 47, 48, position 64, or positions 95, 96, respectively (Figure 2A). These fusion proteins were analyzed by sucrose density gradient ultracentrifugation as described above. The results (Figure 2B) show that GST-ACAT1$_{1-131/P47,48}$ (first row) or GST-ACAT1$_{1-131/P64}$ (second row) exhibits a molecular mass of 70 kDa, thus behaving as a dimer, while GST-ACAT1$_{1-131/P28,29}$ (third row) or GST-ACAT1$_{1-131/P95,96}$ (fourth row) exhibits a molecular mass of 160 kDa, thus behaving as a tetramer. Overall, these results show that inserting proline residues at positions 47, 48 or position 64 disrupts the dimer-forming domain, while inserting proline residues at positions 28, 29 or positions 95, 96 does not produce such an effect. These results narrow down the dimer-forming domain to be within ACAT1 aa 30−94.

Effect of Mutagenizing or Deleting the N-Terminal Peptide on the Oligomerization State of ACAT1. To test the effect of the ACAT1$_{1-101}$ peptide on the oligomerization state of full-length ACAT1, we produced two mutant ACAT1 constructs, HisACAT1/P64, containing proline at aa 64, and HisACAT1/Δ1−65, lacking the first 65 aa of ACAT1. We had previously shown that the His-T7 tag added at the N-terminus of wild-type human ACAT1 does not significantly alter the various biochemical parameters of this enzyme (*33*). Therefore, to provide aid in enzyme purification, each mutant construct contained the His-T7 tag at its N-terminus (*19*). These constructs were expressed in infected H5 cells using procedures described earlier (*16*, *22*, *29*).

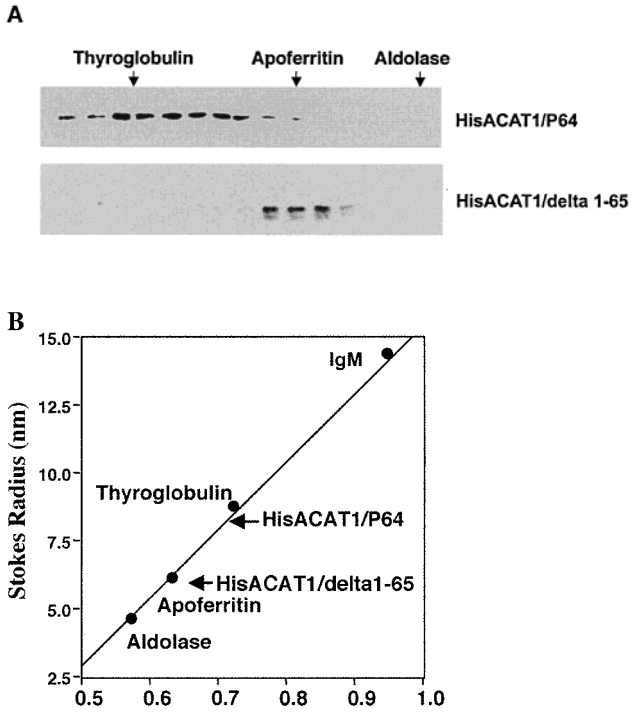

FIGURE 3: (A) Gel filtration chromatography of the HisACAT1/DOC complex using Sepharose CL-6B. Methods for gel filtrations in detergents and for estimating protein molecular masses were according to procedures previously described (*22*). CHAPS-solubilized extracts of wild-type and mutant HisACAT1 cells were used as the enzyme sources. To prepare samples of wild-type and the mutant HisACAT1/DOC complex, one 25 cm^2 flask of insect H5 cells was infected with 25 μL of high titer HisACAT1, HisACAT1/P64, or HisACAT1/Δ1−65 virus for 24 h. Cell lysates were harvested with 1% DOC, 1 M KCl, 10 mM dithiothreitol, 1 mM phenylmethanesulfonyl fluoride, and 0.5 mM leupeptin in buffer A and precleared by ultracentrifugation at 100000*g* for 30 min. 800 μL of the supernatant, with glycerol added to 5% final concentration, was layered onto the column. Proteins of known Stokes radii as indicated were used as standards: aldolase (4.6 nm), apoferritin (6.1 nm), thyroglobulin (8.6 nm), and IgM (13.5 nm); blue dextran 2000 and vitamin B12 were used to determine values for V_0 and V_t, respectively. (B) Stokes radii (R_s) of the mutant HisACAT1/DOC complex. R_s is plotted as a function of the partition coefficient K_{av}. Only the results describing the mutant HisACAT1s were shown. The result using the wild-type HisACAT1 was the same as that reported previously (*22*).

SDS−PAGE Western analysis showed that the wild-type protein and the two different mutant proteins were expressed as undegraded, single molecular species (results not shown). The apparent molecular mass of HisACAT1/P64 is 54 kDa, which is the same as that of the wild-type HisACAT1 (*22*), while the apparent molecular mass of HisACAT1/Δ1−65 is around 46 kDa. Each value is significantly less than the calculated monomeric molecular mass based on their amino acid compositions (69.4 and 61.8 kDa, respectively). Previously, we reasoned that this phenomenon might be related to the high p*I* value and/or the high hydrophobicity of the protein (*29*). Similar to the wild-type HisACAT1, both HisACAT1/P64 and HisACAT1/Δ1−65 remained as integral membrane proteins requiring detergent for solubilization (results not shown). To determine the molecular masses of these mutant proteins, we used deoxycholate- (DOC-) solubilized cell lysates as the enzyme source and then performed gel filtration chromatography (Figure 3A) and sucrose density gradient centrifugation in H_2O and D_2O

Table 1: Hydrodynamic Properties of Wild-Type and Mutant HisACAT1s Determined in DOC[a]

	wild type	P64	Δ1−65
Stokes radius (R_s) (nm)	8.2 ± 0.2	8.1 ± 0.1	6.1 ± 0.1
sedimentation coeff ($s_{20,w}$) (S)	9.6 ± 0.1	8.0 ± 0.1	7.6 ± 0.1
partial specific vol of protein−detergent complex (V_c) (cm^3/g)	0.75	0.75	0.76
partial specific vol of detergent (V_d) (cm^3/g)	0.78	0.78	0.78
mol wt of protein−detergent complex (M_c)	364000 ± 3800	295000 ± 3000	213000 ± 2000
wt fraction of protein in the complex (X_p)	0.77	0.79	0.69
mol wt of protein (M_p)	280000 ± 3000	232000 ± 3000	147000 ± 2000

[a] Calculations were described under Experimental Procedures. Values shown are mean ± SE; $n = 3$.

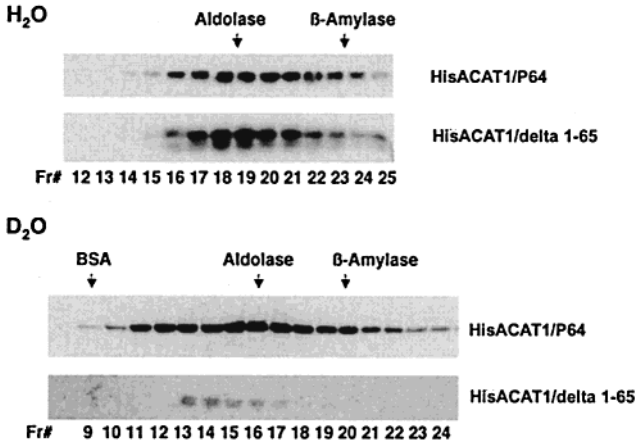

FIGURE 4: Sedimentation profiles of the mutant HisACAT1/DOC complex on sucrose density gradients in H_2O or in D_2O. The experiments were conducted according to procedures previously described (*22*). The enzyme sources were the same as described in Figure 3. Top panel: in H_2O. Bottom panel: in D_2O. Proteins of known sedimentation coefficients were used as standards: bovine serum albumin (4.5), aldolase (7.4), and sweet potato β-amylase (8.9). The peaks of migration of protein standards are as indicated. Only the results describing the mutant HisACAT1s were shown. The result using the wild-type HisACAT1 was the same as that reported previously (*22*).

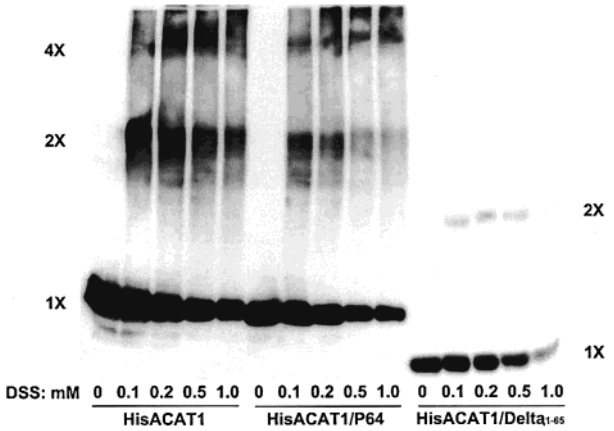

FIGURE 5: Chemical cross-linking of wild-type and mutant HisACAT1s by the primary amine-specific reagent DSS in intact cells. High Five cells were infected with high titer HisACAT1, HisACAT1/P64, or HisACAT1/Δ1−65 recombinant virus for 48 h and cross-linked with DSS at the indicated final concentrations following the procedure previously described (*22*). The sizes of the cross-linked ACAT1 proteins were analyzed by SDS−PAGE under reducing conditions and then visualized by Western blotting using ACAT1-specific antibodies. The symbols 1X, 2X, and 4X indicate that the sizes of the ACAT1-positive signals are 1, 2, or 4 times the size of the ACAT1 monomer on SDS−PAGE. The result shown represents one of three separate experiments.

(Figure 4). The Stokes radii (Figure 3B) and sedimentation coefficients of His-ACAT1, HisACAT1/P64, and HisACAT1/Δ1−65 were determined according to procedures previously established in this laboratory (*22*). The hydrodynamic properties of these three proteins are summarized in Table 1. The results show that both the HisACAT1/DOC complex and the HisACAT1/P64 complex contain approximately 21−23% DOC by weight, while the HisACAT1/Δ1−65 complex contains around 31% DOC by weight. The protein molecular weight of HisACAT1/P64 is estimated at 232000. Since its monomeric molecular mass is 69.4 kDa, this result suggests that HisACAT1/P64 may be either a homotrimer or a homotetramer. The protein molecular weight of HisACAT1/Δ1−65 is estimated at 147000. Since its monomeric molecular mass is 61.8 kDa, this result suggests that HisACAT1/Δ1−65 most likely is a homodimer. The protein molecular weight of HisACAT1 is 280000, confirming the value reported earlier (*22*), and is consistent with the interpretation that HisACAT1 is a homotetramer.

Chemical Cross-Linking of ACAT1. We had previously shown that adding the homobifunctional chemical cross-linking agent to infected insect cells expressing HisACAT1 caused the formation of material up to four times the size of the monomeric enzyme, supporting the conclusion that ACAT1 is a homotetrameric enzyme (*22*). We now use the same method to estimate the oligomeric states of HisACAT1/P64 and HisACAT1/Δ1−65. Figure 5 shows a typical result: adding increasing concentrations of an amine-specific cross-linker disuccinimidyl suberate (DSS) caused an increase in materials two or four times the size of the HisACAT1 or HisACAT1/P64 monomer (first 10 lanes). This result implied that HisACAT1/P64, like HisACAT1, is also a homotetramer. In contrast, the increase in DSS concentration caused the increase in materials two times, but not four times, the size of the HisACAT1/Δ1−65 monomer. When a cysteine-specific cross-linker, bis(maleimidohexane) (BMH), was used, the same result as shown in Figure 5 was obtained (results not shown). These results along with size measurements (summarized in Table 1) support the conclusion that HisACAT1/Δ1−65 is a homodimer.

Enzymatic Properties of HisACAT1, HisACAT1/P64, and HisACAT1/Δ1−65. To investigate the effect of altering ACAT1 from a tetrameric form to a dimeric form, we expressed HisACAT1, HisACAT1/P64, and HisACAT1/Δ1−65 in H5 cells. We then partially purified the three proteins from the detergent-solubilized extracts using metal affinity column chromatography and compared their enzyme activities. To compare the relative activity of these three proteins, we loaded increasing units of enzyme activity produced from HisACAT1, HisACAT1/P64, or HisACAT1/Δ1−65; the relative amount of ACAT1 protein in each preparation was estimated by performing Western blots using

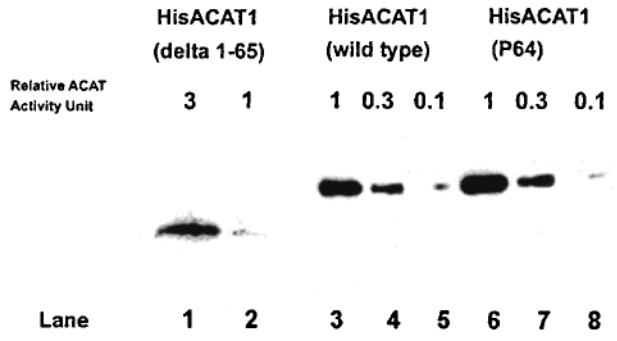

FIGURE 6: Estimation of the relative specific activities of wild-type HisACAT1 (lanes 3−5), HisACAT1/P64 (lanes 6−8), and HisACAT1/Δ1−65 (lanes 1 and 2). The enzymes used were partially purified 20−30-fold from the crude cell extracts by using immobilized metal affinity chromatography (described in detail in Experimental Procedures). The ACAT activities were assayed in taurocholate−PC−cholesterol mixed micelles as previously described (*19*). After ACAT activities were determined for each enzyme type, aliquots that contain known relative ACAT activity units as indicated were added onto each lane. The samples were subjected to analysis by SDS−PAGE. The immunoblotting analysis was performed with T7 monoclonal antibody. The results represent one of three separate experiments.

the T7 monoclonal antibody as the probe. The result shown in Figure 6 indicated that the relative specific activity of HisACAT1/Δ1−65 is approximately five to ten times higher that that of HisACAT1 or HisACAT1/P64. The result of the cholesterol substrate saturation curve experiment (Figure 7A) showed that all three enzymes responded to cholesterol−PC molar ratio (in taurocholate mixed micelles) in a sigmoidal manner. For various allosteric enzymes, the Hill coefficient has been used to determine the degree of cooperativity (p 158 of *34*). We found that the Hill coefficients for HisACAT1, HisACAT1/P64, and HisACAT1/Δ1−65 were very similar (Figure 7B; ranging from 2.51 to 2.75). We next performed oleoyl-coenzyme A substrate saturation curve experiments and found (Figure 8) that all three enzymes responded to oleoyl-coenzyme A concentration hyperbolically; the K_m values were 7.2 μM for both HisACAT1 and HisACAT1/P64 and 15.4 μM for HisACAT1/Δ1−65 ($n = 4$). The rate of heat inactivation in enzyme activity can be a sensitive method to monitor the subtle structural difference(s) between two highly homologous enzymes. We had shown earlier that the rates of activity loss by heat treatment in vitro between the hamster ACAT1 and the human ACAT1 differed significantly (*4*). Using a similar procedure, we monitored the rates of activity loss of these three enzymes after heat treatment at 50 °C; the result (Figure 9) showed that the apparent $t_{1/2}$ of activity loss is approximately 12 min for HisACAT1 and 20 min for HisACAT1/Δ1−65. For HisACAT1/P64, the heat inactivation curve falls between the curves for HisACAT1 and HisACAT1/Δ1−65, and its shape seems to be biphasic. Many ACAT inhibitors of distinct structural types are available (reviewed in ref *2*). On the basis of IC_{50} values, we had earlier shown that human ACAT2, an enzyme highly homologous with human ACAT1 near their C-termini but not near their N-termini, is approximately five times more sensitive to a potent ACAT inhibitor, Dup128, than human ACAT1 (*8*). We monitored the inhibition of HisACAT1, HisACAT1/P64, and HisACAT1/Δ1−65 by Dup128 and found that the IC_{50} values were almost identical to one another: in a typical experiment, the values were 0.13 μM for HisACAT1 and 0.10 μM for both HisACAT1/P64 and HisACAT1/Δ1−65 (Figure 10).

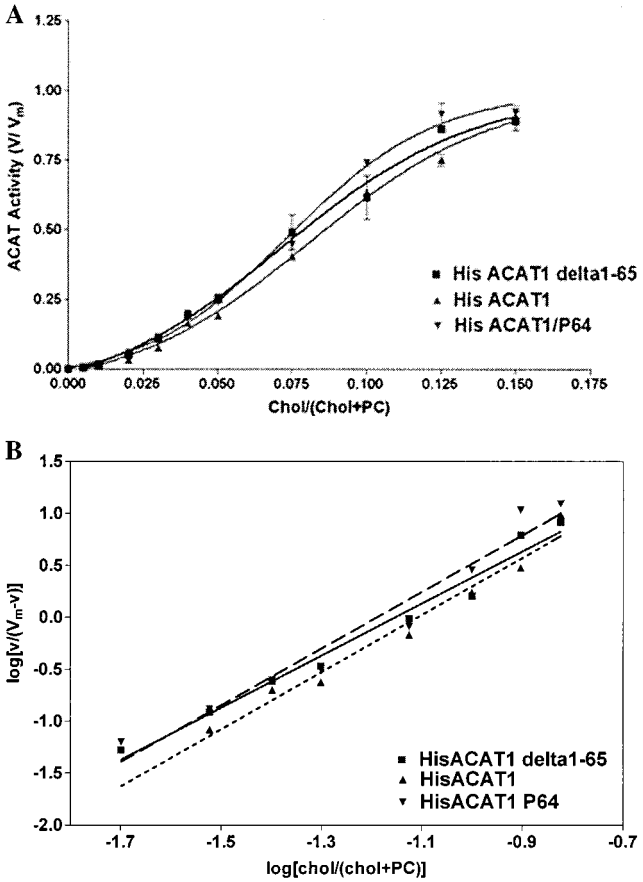

FIGURE 7: (A) Cholesterol substrate saturation curves of HisACAT1 (upward triangle), HisACAT1/P64 (downward triangle), and HisACAT1/Δ1−65 (square). The enzymes used were the same as described in Figure 6. The assay condition was the same as previously described (*19*). For each assay point, 10 μL of partially purified enzyme was added in 50 μL of taurocholate−PC−cholesterol mixed micelles, prechilled at 4 °C, containing taurocholate at 18.6 mM, PC at 9.3 mM, and cholesterol at increasing concentrations as indicated. Values shown were averages of duplicates. To facilitate the comparison among the three enzymes, the ACAT activity values were plotted as V/V_{max}. The V_{max} values were determined by using the software program Prism (GraphPad Software, Inc.). The results represent one of two separate experiments. (B) Hill plots for the cholesterol saturation curves shown in (A) using the program Prism. The Hill coefficient is 2.75 for wild-type HisACAT1, 2.73 for HisACAT1/P64, and 2.51 for HisACAT1/Δ1−65.

DISCUSSION

In this paper, we used the GST fusion protein technology to show that the helical-rich ACAT1 peptide region near the N-terminus contains a specific motif, designated as the dimer-forming motif. When fused with GST, this motif converted the GST protein from a dimer form to a tetramer form. The simplest interpretation of our finding is that this motif forms an intrinsic dimer independent of its fusion protein partner; however, our current data cannot rule out the possibility that this motif interacts with the GST polypeptide and triggers the tetramerization of the GST fusion protein. Further work is needed to distinguish between these two possibilities. The exact location of the dimer-forming motif cannot be pinpointed at present but is in the region between residues 43

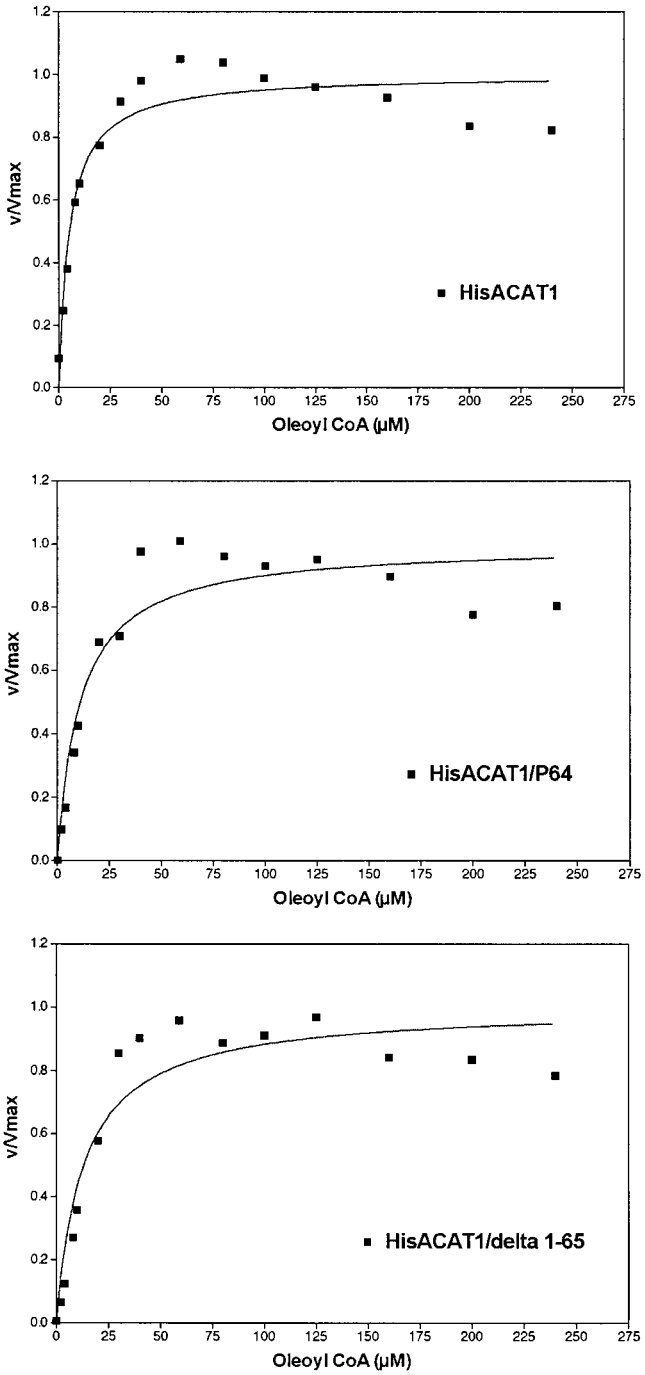

FIGURE 8: Oleoyl-coenzyme A substrate saturation curves of HisACAT1, HisACAT1/P64, and HisACAT1/Δ1−65. The enzyme source was the same as described in Figure 6. The assay condition was essentially the same as previously described with minor modification (*19*). Each assay tube contained 17.7 μL of protein and 138.3 μL of mixed micelles with taurocholate at 18.6 mM, phosphatidylcholine at 11.2 mM, and cholesterol at 1.6 mM (with ^{3}H label at 4.6×10^6 dpm). The reaction was initiated by adding 22.3 μL of assay mixture containing oleoyl-CoA at the indicated final concentrations premixed with fatty acid-free bovine serum albumin at an equal molar ratio. The result shown represents one of four separate experiments.

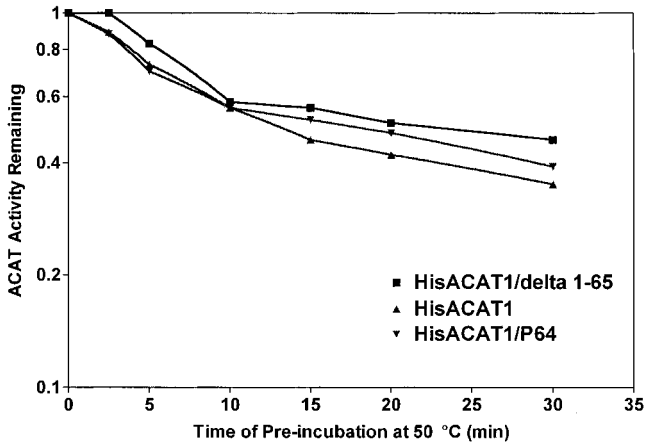

FIGURE 9: Heat inactivation of wild-type and mutant ACAT1 enzymes. The enzyme source was the same as described in Figure 6. 20 μL of partial purified HisACAT1 enzymes was added to 100 μL of mixed micelles (described in Figure 8), and the mixture was incubated at 50 °C for various times as indicated. At each indicated time point, the enzyme−micelle mixture was cooled on ice. The ACAT activity assay was initiated by the addition of 20 μL of assay mixture as previously described (*19*). Assay was carried out at 37 °C for 15 min. The results shown represent one of three separate experiments.

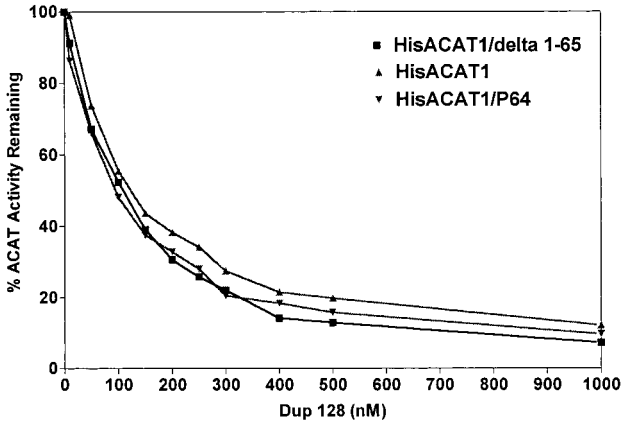

FIGURE 10: Sensitivity of wild-type and mutant ACAT1 enzymes toward an ACAT inhibitor Dup128. The enzyme source was the same as described in Figure 6. 20 μL of individual HisACAT1 enzyme as indicated was added to 100 μL of taurocholate−PC−cholesterol micelles, and the mixture was incubated with the specific ACAT inhibitor Dup128 at different final concentrations as indicated for 5 min on ice. 20 μL of the assay mixture was then added to start the ACAT reaction. Assay was carried out at 37 °C for 20 min. The results shown represent one of three separate experiments.

and 84 (Figure 2). We arrive at this conclusion on the basis of results indicating that this motif could be disrupted by the P47,48 or the P64 mutation but not by the P28 or the P95,96 mutations. Of interest, two putative leucine zipper-like motifs may exist within the regions that comprise aa 47−61 and aa 80−94 (*4*). Leucine zipper motifs can mediate protein−protein interactions and form dimers, trimers, and tetramers (*35*, *36*). In the future, the structure of this motif can be solved by X-ray crystallography combined with site-specific mutagenesis. Additional results showed that the single substitution mutation (P64) within the full-length ACAT1 caused a significant decrease in the sedimentation coefficient and a significant decrease in its apparent protein molecular weight (Table 1), but it was not able to change the protein from a tetramer to a dimer. Instead, we found that, by deleting part of the dimer-forming motif, we were able to convert the enzyme from a homotetramer (HisACAT1) to a homodimer (HisACAT1/Δ1−65). These results raise the possibility that, other than the dimer-forming motif located between aa residues 43 and 84, additional interaction(s) may occur between the N-terminal peptide segment and

the rest of the polypeptide chain to reinforce the tetramer formation. Interestingly, we found that the dimeric form is five to ten times more active than the tetrameric form. Other enzymatic properties of the dimeric form, including the K_m value for oleoyl-CoA, the rate of heat inactivation, and sensitivity toward a specific ACAT inhibitor Dup128, were almost unaltered from those of the tetrameric form. We also found that reducing the oligomeric structure of the enzyme from a tetramer to a dimer did not alter the sigmoidal cholesterol substrate saturation curve. This result shows that the tetrameric form is not required for ACAT1 to behave as an allosteric enzyme.

It is possible that ACAT1 may exist as a twofold dimer; namely, the homodimeric unit may be the minimal functional unit required to express enzyme activity and to exhibit cooperativity toward cholesterol. It is also possible that, even in monomeric form, ACAT1 may still be catalytically active and may still behave as an allosteric enzyme. In the future, to distinguish between these two possibilities, it will be necessary to further dissociate the enzyme from the dimeric form to the monomeric form. We had previously shown that ACAT1s in vitro and in intact cells mainly exist as homotetramers. This conclusion was mainly based on results from transfection studies. Our current work shows that the dimeric form is catalytically much more active than the tetrameric form. Therefore, it is possible that a dimeric form of ACAT1 may exist under certain physiological stimuli, particularly under conditions that call for a large increase in intracellular cholesterol esterification. This possibility will be investigated in the future.

ACKNOWLEDGMENT

We thank Dong Cheng, Trista North, and Justin Hart for participating in certain stages of this work and Helina Morgan for careful editing of the manuscript.

REFERENCES

1. Chang, T. Y., Chang, C. C. Y., and Cheng, D. (1997) *Annu. Rev. Biochem. 66*, 613−638.
2. Krause, B. R., and Bocan, T. M. A. (1995) in *Inflammation: Mediators and pathways* (Ruffolo, R. R., Jr., and Hollinger, M. A., Eds.) pp 173−198, CRC Press, Boca Raton, FL.
3. Puglielli, L., Konopka, G., Pack-Chung, E., MacKenzie Ingano, L. A., Berezovska, O., Hyman, B. T., Chang, T. Y., Tanzi, R. E., and Kovacs, D. M. (2001) *Nat. Cell Biol. 3*, 905−912.
4. Chang, C. C. Y., Huh, H. Y., Cadigan, K. M., and Chang, T. Y. (1993) *J. Biol. Chem. 268*, 20747−20755.
5. Anderson, R. A., Joyce, C., Davis, M., Reagan, J. W., Clark, M., Shelness, G. S., and Rudel, L. L. (1998) *J. Biol. Chem. 273*, 26747−26754.
6. Cases, S., Novak, S., Zheng, Y. W., Myers, H., Lear, S. R., Sande, E., Welch, C. B., Lusis, A. J., Spencer, T. A., Krause, B. R., Erickson, S. K., and Farese, R. V., Jr. (1998) *J. Biol. Chem. 273*, 26755−26764.
7. Oelkers, P., Behari, A., Cromley, D., Billheimer, J. T., and Sturley, S. L. (1998) *J. Biol. Chem. 273*, 26765−26771.
8. Chang, C. C. Y., Sakashita, N., Ornvold, K., Lee, O., Chang, E., Dong, R., Lin, S., Lee, C. Y. G., Strom, S., Kashyap, R., Fung, J., Farese, R., Jr., Patoiseau, J. F., Delhon, A., and Chang, T. Y. (2000) *J. Biol. Chem. 275*, 28083−28092.
9. Lee, O., Chang, C. C. Y., Lee, W., and Chang, T. Y. (1998) *J. Lipid Res. 39*, 1722−1727.
10. Sakashita, N., Miyazaki, A., Takeya, M., Horiuchi, S., Chang, C. C. Y., Chang, T. Y., and Takahashi, K. (2000) *Am. J. Pathol. 156*, 227−236.
11. Chang, T. Y., Chang, C. C. Y., Lin, S., Yu, C., Li, B. L., and Miyazaki, A. (2001) *Curr. Opin. Lipidol. 12*, 289−296.
12. Seo, T., Oelkers, P. M., Giattina, M. R., Worgall, T. S., Sturley, S. L., and Deckelbaum, R. J. (2001) *Biochemistry 40*, 4756−4762.
13. Rudel, L., Lee, R., and Cockman, T. (2001) *Curr. Opin. Lipidol. 12*, 121−127.
14. Cao, G., Goldstein, J. L., and Brown, M. S. (1996) *J. Biol. Chem. 271*, 14642−14648.
15. Hofmann, K. (2000) *Trends Biochem. Sci. 25*, 111−112.
16. Lu, X., Lin, S., Chang, C. C. Y., and Chang, T. Y. (2002) *J. Biol. Chem. 277*, 711−718.
17. Chang, T. Y., Chang, C. C. Y., Lu, X. H., and Lin, S. (2001) *J. Lipid Res. 42*, 1933−1938.
18. Guo, Z., Cromley, D., Billheimer, J. T., and Sturley, S. L. (2001) *J. Lipid Res. 42*, 1282−1291.
19. Chang, C. C. Y., Lee, C. Y., Chang, E. T., Cruz, J. C., Levesque, M. C., and Chang, T. Y. (1998) *J. Biol. Chem. 273*, 35132−35141.
20. Lin, S., Cheng, D., Liu, M. S., Chen, J., and Chang, T. Y. (1999) *J. Biol. Chem. 274*, 23276−23285.
21. Joyce, C. W., Shelness, G. S., Davis, M. A., Lee, R. G., Skinner, K., Anderson, R. A., and Rudel, L. L. (2000) *Mol. Biol. Cell 11*, 3675−3687.
22. Yu, C., Chen, J., Lin, S., Liu, J., Chang, C. C. Y., and Chang, T. Y. (1999) *J. Biol. Chem. 274*, 36139−36145.
23. Rost, B., and Sander, C. (1993) *J. Mol. Biol. 232*, 584−599.
24. Rost, B., and Sander, C. (1994) *Proteins 19*, 55−72.
25. Sargiacomo, M., Scherer, P., Tang, Z., Kubler, E., Song, K. S., Sanders, M. C., and Lisanti, M. P. (1995) *Proc. Natl. Acad. Sci. U.S.A. 92*, 9407−9411.
26. Pearce, S. F. A., Wu, J., and Silverstein, R. L. (1995) *J. Biol. Chem. 270*, 2981−2986.
27. Chang, C. C. Y., Chen, J., Thomas, M. A., Cheng, D., Del Priore, V. A., Newton, R. S., Pape, M. E., and Chang, T. Y. (1995) *J. Biol. Chem. 270*, 29532−29540.
28. Sambrook, J., Fritsch, E. F., and Maniatis, T. (1989) *Molecular Cloning: A Laboratory Manual*, Cold Spring Harbor Laboratory, Cold Spring Harbor, NY.
29. Cheng, D., Chang, C. C. Y., Qu, X. M., and Chang, T. Y. (1995) *J. Biol. Chem. 270*, 685−695.
30. Chang, T. Y., Limanek, J. S., and Chang, C. C. Y. (1981) *Anal. Biochem. 116*, 298−302.
31. Smith, D. B., and Johnson, K. S. (1988) *Gene 67*, 31−40.
32. Letai, A., Coulombe, P. A., and Fuchs, E. (1992) *J. Cell Biol. 116*, 1181−1195.
33. Chang, C. C. Y., Lee, C. Y. G., Chang, E. T., Cruz, J. C., Levesque, M. C., and Chang, T. Y. (1998) *J. Biol. Chem. 273*, 35132−35141.
34. Stryer, L. (1995) *Biochemistry*, 4th ed., Freeman and Co., New York.
35. Landschultz, W. H., Johnson, P. F., and McKnight, S. L. (1988) *Science 243*, 1681−1688.
36. Patel, S., and Hingorani, M. (1993) *J. Biol. Chem. 268*, 10668−10675.

BI0120188